



## Article

# *LvbHLH13* Regulates Anthocyanin Biosynthesis by Activating the *LvMYB5* Promoter in Lily (*Lilium* 'Viviana')

Wenzhong An <sup>1,†</sup>, Yibo Sun <sup>1,†</sup>, Zhenhua Gao <sup>1,†</sup>, Xiaoye Liu <sup>1</sup>, Qi Guo <sup>1</sup>, Shaokun Sun <sup>2</sup>, Minghui Zhang <sup>1</sup>, Yutong Han <sup>1</sup>, Muhammad Irfan <sup>3</sup> , Lijing Chen <sup>1,\*</sup> and Di Ma <sup>1,\*</sup>

- <sup>1</sup> Key Laboratory of Agriculture Biotechnology of Liaoning Province, College of Biosciences and Biotechnology, Shenyang Agricultural University, Shenyang 110866, China; anwenzhong2019@stu.syau.edu.cn (W.A.); sunyibo0361@163.com (Y.S.); gaozhenhua@stu.syau.edu.cn (Z.G.); liuxiaoye@stu.syau.edu.cn (X.L.); guoqi@stu.syau.edu.cn (Q.G.); zhangminghui@stu.syau.edu.cn (M.Z.); hanyutong@stu.syau.edu.cn (Y.H.)
- <sup>2</sup> Institute of Vegetable Research, Liaoning Academy of Agricultural Sciences, Shenyang 110161, China; sunshaokun2015@126.com
- <sup>3</sup> Department of Biotechnology, University of Sargodha, Sargodha 40100, Pakistan; irfan.ashraf@uos.edu.pk
- \* Correspondence: chenlijing1997@126.com (L.C.); madi@syau.edu.cn (D.M.); Tel.: +86-024-88487163 (L.C.); Fax: +86-024-88492799 (D.M.)
- † These authors should be considered co-first authors.

**Abstract:** Anthocyanins, constituents of flavonoid compounds prevalent in plants, possess significant value in both plant development and human nutrition. The regulation of anthocyanin biosynthesis primarily involves the orchestration of MYB, bHLH, and WD40 transcription factors. Consequently, the bHLH family assumes a pivotal role in modulating plant developmental processes. In the present investigation, a transcription factor, denoted as *LvbHLH13*, was identified as a positive regulator of anthocyanin pigmentation in lily petals. *LvbHLH13* is classified within the IIIId subgroup of *Arabidopsis* bHLH proteins. Functional analyses involving the transient expression and gene silencing of *LvbHLH13* revealed its capacity to enhance and diminish anthocyanin accumulation, respectively, by modulating the *LvMYB5* expression, thereby influencing the downstream structural gene expression. The overexpression of *LvbHLH13* resulted in an increase in the expression of the downstream structural genes related to anthocyanin synthesis, whereas silencing of *LvbHLH13* correspondingly decreased the expression. Yeast one-hybrid and EMSA assays demonstrated the interaction between *LvbHLH13* and the *LvMYB5* promoter, leading to the activation of anthocyanin biosynthesis. A further luciferase (LUC) analysis corroborated the stimulatory effect of *LvbHLH13* on the *LvMYB5* promoter sequence. Consequently, *LvbHLH13* assumed a crucial role in lily-petal pigmentation. A yeast two-hybrid analysis revealed that *LvbHLH13* diverged from typical bHLH transcription factor behavior as it did not form a complex with MYB to regulate anthocyanin biosynthesis. This discrepancy could be attributed to the deletion of the N-terminal conserved sequence of *LvbHLH13*. This study provides a new bHLH candidate and bHLH-MYB partner to explore the anthocyanin regulatory network in further research and provides new opportunities for breeding lilies with various anthocyanin contents. These findings lay a theoretical foundation for subsequent investigations into lily flower coloring mechanisms.

**Keywords:** lily; anthocyanins; *LvbHLH13*; *LvMYB5*; protein–nucleic acid interaction; protein interaction



**Citation:** An, W.; Sun, Y.; Gao, Z.; Liu, X.; Guo, Q.; Sun, S.; Zhang, M.; Han, Y.; Irfan, M.; Chen, L.; et al. *LvbHLH13* Regulates Anthocyanin Biosynthesis by Activating the *LvMYB5* Promoter in Lily (*Lilium* 'Viviana'). *Horticulturae* **2024**, *10*, 926. <https://doi.org/10.3390/horticulturae10090926>

Received: 17 July 2024

Revised: 19 August 2024

Accepted: 19 August 2024

Published: 30 August 2024



**Copyright:** © 2024 by the authors. Licensee MDPI, Basel, Switzerland. This article is an open access article distributed under the terms and conditions of the Creative Commons Attribution (CC BY) license (<https://creativecommons.org/licenses/by/4.0/>).

## 1. Introduction

The lily has captivated human affection for centuries. These flowers are not just aesthetically pleasing, but they also play significant roles in various fields, including horticulture, floriculture, medicine, and symbolism. The range of lily flower colors spans from pristine white to vibrant pinks, oranges, and even near-black hues. Each hue carries biological importance, with color being an essential factor in attracting pollinators and ensuring successful reproduction [1–4]. During the pigment accumulation of plants, flavanols and

anthocyanins have attracted particular attention because they are responsible for not only rendering most colors and preventing biotic and abiotic damage in plants but also the health benefits for humans [5–7]. Due to their high antioxidant activity, anthocyanins have been linked to the prevention of several chronic diseases [8].

Anthocyanins, which are part of flavonoid compounds, are synthesized through a complex pathway regulated transcriptionally by a set of interconnected genes [9–12]. These genes encompass chalcone synthase (CHS), chalcone isomerase (CHI), flavanone 3-hydroxylase (F3H), and flavonoid 3'-hydroxylase (F3'H), responsible for generating common precursors. Further downstream in the pathway are genes like flavonoid-3-O-glucosyltransferase (3GT), anthocyanidin synthase (ANS), and dihydroflavonol-4-reductase (DFR) [13–15], typically considered to be late biosynthetic genes (LBGs). In lilies, the expression of DFR, ANS, and 3GT is intimately linked to color formation. The regulatory transcription factors (TFs) controlling these genes consist of MYB TFs, bHLH TFs, and MYB-bHLH-WD40 (MBW) complexes, composed of MYB, bHLH, and WD40 repeat proteins [4,9,11,16–19].

Recent investigations have increasingly shed light on the role of numerous bHLH TFs in governing the flavonoid pathway [20–24]. Strawberry R2R3-*FaMYB5* interacts with *FaEGL3* and *FaLWD1* to form a MBW complex, which positively regulates the accumulation of anthocyanin through the activation of F3'H [25]. *HvnAnt2* interacts with flavonoid 3'-monooxygenase, anthocyanin biosynthesis gene regulators, and key enzymes in folate metabolism, which play a role in the formation of different qingke barley-grain colors [26]. Another study suggested that *ThRAX2* may pass through a specific recognition of the MYB-T motif to enhance Cd tolerance to regulate the downstream expression and also regulate anthocyanidin synthase protein transport and activity [27]. The bHLH TFs have been extensively studied, with an increasing focus on their involvement in the response to environmental factors such as cold temperatures, salt, drought, and iron deficiency [28]. Another bHLH factor, inducer of C-repeat binding factor expression 2 (ICE2), acts antagonistically to control seed dormancy by regulating the ABA catabolism gene *ABA8OX3* in a temperature-dependent manner [29]. The above studies indicate the different functions of bHLH TFs in different plants.

In the genome of *Arabidopsis thaliana*, 32 families of bHLH genes encode TFs with three or more branches [30], each featuring a crucial helix-loop-helix structural domain essential for homodimer or heterodimer formation [15]. This domain exhibits a highly conserved amino acid sequence, typically encompassing the DNA binding domain. The majority of group III members function as TFs governing flavonoid-metabolism genes, illustrated by TT8 (TRANSPARENT TESTA8), GL3 (GLABRA3), and EGL3 (ENHANCER OF GLABRA3), which regulate anthocyanin synthesis in *Arabidopsis thaliana* [31–33]. TT8, a significant bHLH transcription factor in anthocyanin regulation, primarily oversees DFR expression in seedlings and pods and plays a role in MBW complex assembly. However, compared with III f subgroup bHLH TFs, in III d subgroups, a segment of amino acids is mutated. The N-terminal conservatism of the III d subgroup is considered to be an important factor regulating anthocyanin accumulation [3,4,34]. Conversely, MYB genes constitute another class of regulators not involved in MBW complexes. MYBs related to flavonoid function typically bind to the promoters of target structural genes to initiate expression, relying on interaction with bHLHs for this binding mechanism [35,36]. Research on the gene regulatory network governing anthocyanin production in lilies is notably scarce, especially when contrasted with studies conducted in model plants. [37]. The previous study showed that *LvMYB5* could activate anthocyanin synthesis by interacting with structural genes [37]. The content of anthocyanins was positively correlated with the transcript abundance of *LvMYB5*. The results suggested that *LvMYB5* controlled anthocyanin biosynthesis together with its regulator partner, bHLH. Unfortunately, the bHLH partner of *LvMYB5* in lily has not reported. So, it is necessary to identify lily anthocyanin regulatory factors and lay a basis for the breeding of highly gorgeous and high-anthocyanin lilies.

In this study, a bHLH TF was identified through transcriptome sequencing, and subsequent expression verification revealed that *LvbHLLH13* exhibited a similar expression pattern to that of early anthocyanin structural genes. Transient overexpression and virus-induced gene silencing (VIGS) experiments were then conducted, demonstrating that *LvbHLLH13* plays a regulatory role in modulating anthocyanin biosynthesis by influencing the expression of *LvMYB5* and structural genes. To further validate the functionality of these gene-encoded proteins and elucidate the interaction between *LvMYB5* and *LvbHLLH13*, yeast one-hybrid assays, electrophoretic mobility shift assay (EMSA), dual-luciferase assay (LUC), and subcellular localization were conducted. The findings of this study revealed the molecular regulatory mechanism of bHLH genes in lily color formation, contributing to a deeper understanding of anthocyanin biosynthesis and flower color development.

## 2. Materials and Methods

### 2.1. Materials

The cultivar was used as previously described [7]. In 2022, the plants were cultivated in a greenhouse at Shenyang Agricultural University, where temperatures fluctuated between 2 and 25 degrees Celsius.

Samples were separated manually into three groups according to the growing stage: the bud stage (S1), the coloring stage (S2), and the full-blooming stage (S3). In S3, the unpigmented region of the petal was marked as X. All samples were collected and immediately frozen in liquid nitrogen and stored at  $-80^{\circ}\text{C}$  for further analysis. *Nicotiana benthamiana* seedlings at 4–6 weeks of age were used in the experiments.

### 2.2. RNA Extraction, cDNA Synthesis, and qRT-PCR

An RNA extraction kit (Biolab, Beijing, China) was utilized following the manufacturer's instructions. RNA integrity was evaluated via 1.0% agarose gel electrophoresis, while purity was determined by the A260/A280 absorption ratio using a spectrophotometer (BIODROP, Cambridge, UK). Subsequently, 1 mg of total RNA from each sample was reverse-transcribed into cDNA using the PrimeScript™ RT kit (Monad, Suzhou, China) following the manufacturer's protocols. The resulting cDNA was diluted tenfold with ddH<sub>2</sub>O and employed as a template for quantitative real-time PCR (qRT-PCR).

The reaction was carried out with a 1 mL volume mixture containing 100  $\mu\text{L}$  of cDNA (50 ng/ $\mu\text{L}$ ), 30  $\mu\text{L}$  of each forward and reverse primers (10 pmol/ $\mu\text{L}$ ), 500  $\mu\text{L}$  of Mon-Amp™ ChemoHS qPCR SYBR Green SuperMix (Monad, Suzhou, China), and 340  $\mu\text{L}$  of ddH<sub>2</sub>O. The steps are as follows: pre-denaturation,  $95^{\circ}\text{C}$  10min; denaturation,  $95^{\circ}\text{C}$  10 s; renaturation,  $60^{\circ}\text{C}$  30 s; extension phase,  $72^{\circ}\text{C}$  30 s; for a total of 40 cycles. Quantitative analysis of anthocyanin-related genes was conducted using qRT-PCR with three biological replicates and a technical replicate. The reference gene actin was employed for normalization purposes. Relative gene expression levels were determined using the  $2^{-\Delta\Delta\text{Ct}}$  method, where  $\Delta\text{Ct} = \text{Ct}(\text{target gene}) - \text{Ct}(\text{actin})$ . Gene-specific primers were designed utilizing the NCBI web tool Primer-BLAST <https://blast.ncbi.nlm.nih.gov/Blast.cgi> (accessed on 14 May 2023), ensuring product sizes within the range of 100 to 200 bp. Further details on the anthocyanin genes and the primers used are provided in Supplementary Table S1.

### 2.3. Anthocyanin Concentration Analysis

The anthocyanin concentrations were determined according to references [37–40]. Briefly, 0.1 g of the ground sample powder was added to 700  $\mu\text{L}$  of methanol extraction buffer (1% HCl) at  $4^{\circ}\text{C}$ , and the mixture was incubated overnight. Then, 400  $\mu\text{L}$  of ddH<sub>2</sub>O and 400  $\mu\text{L}$  of chloroform were added sequentially to extract chlorophyll. Centrifugation was performed (Thermo Scientific, Waltham, MA, USA) at  $14,000\times g$  at  $4^{\circ}\text{C}$  for 5 min to obtain anthocyanin supernatants. Absorption values were measured at 530 nm and 657 nm (Thermo Scientific, Evolution™ 350, USA). Finally, we calculated the anthocyanin content of the plant using the formula  $A_{530} - 0.33A_{657}$ . For each sample, three replicates were extracted and measured. The analysis was carried out using the SPSS16.0 software package.

#### 2.4. Virus-Induced Gene Silencing (VIGS) of *LvMYB5* and *LvbHLH13* Genes in Lily Petals

A 250 bp fragment was amplified from specific regions of *LvMYB5* (*LvMYB5*-TRV2) and *LvbHLH13* (*LvbHLH13*-TRV2) with *EcoR* I and *Xho* I inserted by the 5' end of the forward and reverse primers, respectively (Supplemental Table S1). The target segment was cloned into the pTRV2 vector, resulting in recombinant plasmids pTRV2-*LvMYB5* and pTRV2-*LvbHLH13*. These recombinant plasmids were subsequently introduced into *Escherichia coli* DH5 $\alpha$ , and positive clones were selected for DNA sequencing to verify the integrity and accuracy of the inserted sequences [41].

Three groups (pTRV1 + pTRV2, pTRV1 + pTRV2-*LvMYB5*, and pTRV1 + pTRV2-*LvbHLH13*) were cultured in an LB medium supplemented with 25 mg/L rifampin and 50 mg/L kanamycin at 28 °C until reaching an optical density at 600 nm (A600) of 0.8–1.0, measured using a spectrophotometer. The cells were then centrifuged into pellets and resuspended in a buffer solution containing 10 mM MES, 10 mM MgCl<sub>2</sub>, and 150 mM acetosyringone at pH 5.6, with the A600 adjusted to 0.8. The resuspended cells were then incubated for 3 h at room temperature in the dark. Prior to infiltration, each group received an equivalent volume of *Agrobacterium* cultures harboring pTRV1 and pTRV2 vectors.

The mixture was injected into the outer petals at the S2 stage using a 1 mL needle-free syringe. Six biological replicates were used per treatment. Phenotypic identification was carried out in a growth chamber with the following settings: 25 °C, 60% humidity, and 16 h light–8 h dark. After treatment in the dark for 24 h, the growth chamber was subjected to a 16 h light–8 h dark cycle; photographs were taken after 6 days.

#### 2.5. Overexpression of *LvMYB5* and *LvbHLH13* Genes in Lily Petals

In the presence of 35S promoter control, the cDNA of *LvbHLH13* was cloned to the pCAMBIA1300-GFP vector between *Bam*H I and *Sal* I via homologous recombination. Then, using the freeze-thaw method, the recombinant plasmid was transformed into a single-cell strain of *Agrobacterium tumefaciens*. The plasmid was incubated at 28 °C for 48 h. Finally, the expression vector named 35S::*LvbHLH13* was obtained. The sequence of the primers used is provided in Supplementary Table S1.

#### 2.6. Subcellular Localization of *LvMYB5* and *LvbHLH13*

The coding sequences (CDSs) of *LvMYB5* and *LvbHLH13* were cloned into the *Bam*H I and *Sal* I restriction sites of the pCAMBIA1300-GFP vector, resulting in *LvMYB5*-GFP and *LvbHLH13*-GFP constructs. Both the control and recombinant vectors were then injected into *Nicotiana benthamiana* leaves through agroinfiltration, following the established protocols [7]. After an incubation period of 72 h (including 24 h in the dark), fluorescence was observed using a confocal laser scanning microscope, as described previously [42]. Details of the primers are listed in Supplementary Table S1.

#### 2.7. Yeast One-Hybrid Assay of *LvbHLH13* and *LvMYB5* Promoter

Three deletion fragments of MYBp (2000+ bp), namely, MYBp1 (1200 bp), MYBp2 (900 bp), and MYBp4 (300 bp), were inserted into the *Xho* I and *Sac* I sites in the pAbAi vector. Subsequently, pAbAi-*LvMYB5* and pGADT7-*LvbHLH13* were co-transformed into yeast cells (Y1H) following the provided instructions.

#### 2.8. Electrophoretic Mobility Shift Assay (EMSA) of *LvbHLH13* and *LvMYB5* Promoter

The coding sequence (CDS) of *LvbHLH13* was cloned into the pGEX6P vector and subsequently introduced into DE3 Rosetta Competent cells. Following induction with 0.5 mM IPTG, the recombinant *LvbHLH13*-His tag protein was purified using a GST-tag Protein Purification Kit (Beyotime, Shanghai, China) according to the manufacturer's instructions. Subsequently, the purified protein was subjected to 8% SDS-PAGE for isolation. In the EMSA (Electrophoretic Mobility Shift Assay), three labeled DNA probes containing the G-box from the upstream promoter sequence of *LvMYB5* were employed for detection. Unlabeled probes were used as competitors. The EMSAs were performed using a chemilu-

minescent EMSA Kit (Beyotime, Shanghai, China). Details of the primers are presented in Supplementary Table S1.

### 2.9. Dual-Luciferase Transient Assay

A 2000 bp *LvMYB5* upstream promoter sequence was inserted into a pGreenII-0800-LUC vector to construct the reporter vector *LvMYB5* pro-LUC. The CDS sequence of *LvbHLH13* was cloned into the 35S:: GFP vector (pGreenII-62-SK). The effector vectors, including *LvbHLH13*-62-SK and the empty vector pGreenII-62-SK, were utilized in this study. The *A. tumefaciens* reporter and effector strains were co-transformed into 4-week-old tobacco (*N. benthamiana*) leaves using previously described methods [43].

For the detection of luciferase (LUC) activity, a Dual-Luciferase Reporter Assay System (Promega) was used. The primer sequences are listed in Supplementary Table S1.

### 2.10. Yeast Two-Hybrid Assay of *LvbHLH13* and *LvMYB5* Promoter

The CDS sequences of *LvbHLH13* and *LvMYB5* were inserted into the *EcoR* I/*Bam* H I sites of the pGADT7 vector and the *EcoR* I/*Pst* I sites of the pGBKT7 (BD) vector, respectively. pGADT7-*LvbHLH13* and pGBKT7-*LvMYB5* constructs were then co-transformed into yeast cells (Y2H), following the protocol's instructions. The CDS sequence of 53 was cloned into the pGBKT7 vector (resulting in pGBKT7-53), co-transformed with pGADT7-T, and used as a positive control. The transformed yeast cells were initially cultured in a medium without tryptophan and leucine (–T/–L) and subsequently transferred to a medium containing aureobasidin A (ABA), tryptophan, leucine, histidine, and adenine (–T/–L/–H/–A) for further analysis.

### 2.11. Statistical Measurement

All statistical data were analyzed using ANOVA with Tukey's correction according to the study by Sun. Different letters indicate significant differences ( $p < 0.05$ ) in the least significant difference (LSD) test or Student's *t*-test (\*  $p$ -value  $< 0.05$ , \*\*  $p$ -value  $< 0.01$ , \*\*\*  $p$ -value  $< 0.001$ ) [40].

## 3. Results

### 3.1. Spatiotemporal Differences in Gene Expression during Anthocyanin Accumulation in Lily Petals

Figure S2 illustrates the results of the identification of the bHLH transcription factor family using the lily transcriptome and genomic databases. The open reading frames (ORFs) of *LvbHLH13*-encoded proteins consisted of 544 amino acids, with the MYB interaction domain located in the N-terminal region, similar to other bHLH transcription factor proteins associated with plant anthocyanin production. Based on the color change observed in lily petals (Figure 1A), samples were collected at three flowering stages, namely, the bud stage (S1), the coloring stage (S2), and the full blooming stage (S3), along with unpigmented petal samples (X). As depicted in Figure 1B, extracts with the same dilution ratio displayed a progressive deepening of color from white to purple throughout the petal development. At each stage, the total anthocyanin content of the petals was determined. The results revealed that S1 petals, corresponding to the white extract, exhibited a significantly lower anthocyanin content than the samples from the other two stages. Anthocyanin accumulation markedly increased from 0.04 mg/g (S1) to 3.82 mg/g (S3) as the petals began to exhibit coloration (Figure 1B). Hence, the variation in the anthocyanin content in petals suggests a gradual accumulation of anthocyanins during flower development.

To examine the genes associated with the color of lilies, the transcription factor (TF) *LvbHLH13* (GeneBank accession no. PP442030) was isolated and cloned to analyze the gene expression at different developmental stages. Following a previous study [37], the anthocyanin-related structural genes *LvCHS*, *LvF3H*, *LvDFR*, *Lv3GT*, and *LvANS*, as well as the positive transcriptional regulator *LvMYB5*, were cloned from lily. qRT-PCR was performed to quantitatively analyze the gene expression in the different stages. The results

are shown in Figure 1C. *LvMYB5* was upregulated in S2 and S3, and most of the late structural genes also revealed increased expression during flower development. Moreover, compared to the pigmented section (S3), the unpigmented zone (X) had a substantially lower concentration of cyanidin derivatives (Figure 1C), which can be attributed to anthocyanin accumulation. However, the expression of *LvbHLLH13* was highest in the S1 period, slightly downregulated in the S2 period, and significantly downregulated in the S3 period. This is consistent with changes in early anthocyanin biosynthesis genes, indicating that *LvbHLLH13* is mainly expressed during the early stage of anthocyanin accumulation. Therefore, *LvbHLLH13* and *LvMYB5* show spatiotemporal differences in the expression of petal color accumulation, suggesting that *LvbHLLH13* may be upstream of *LvMYB5*, and they could have opposing effects on anthocyanin synthesis and/or accumulation.

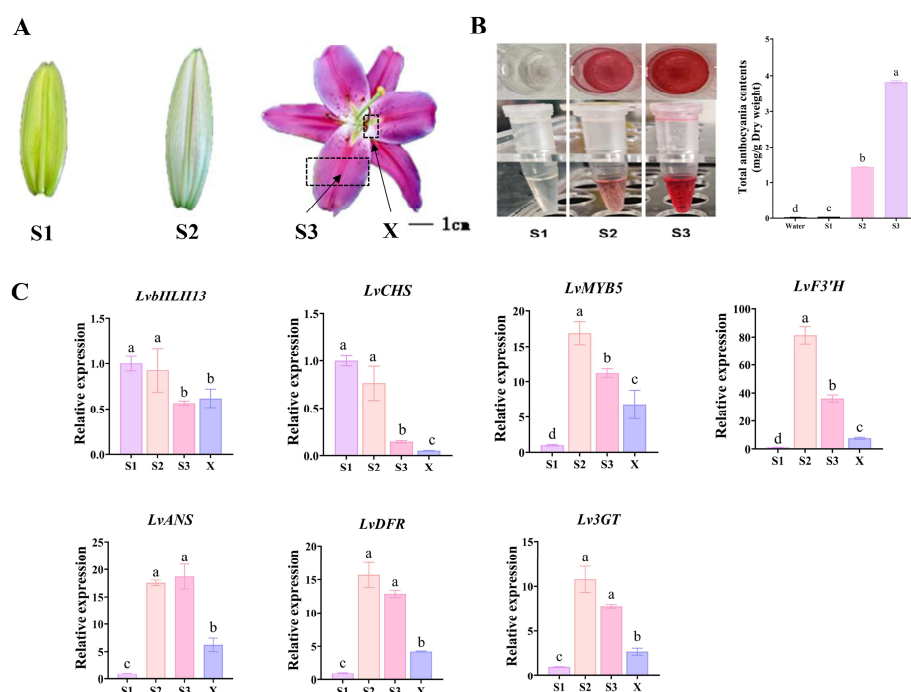


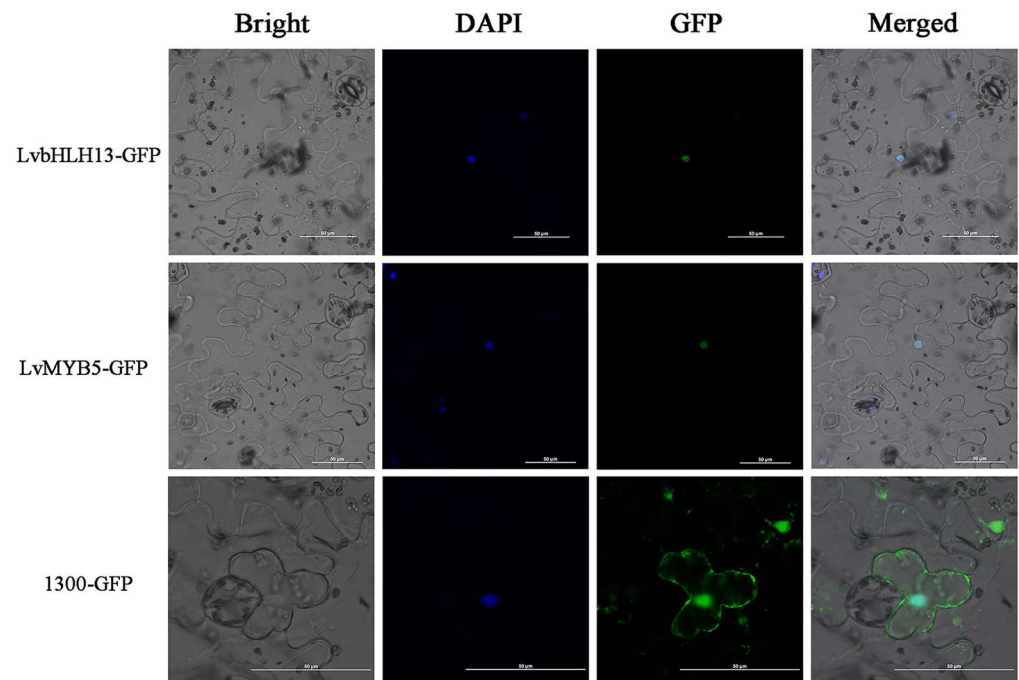
**Figure 1.** Investigating anthocyanin content and analyzing *LvMYB5*, *LvbHLLH13*, and associated structural genes' expression during lily development. (A) Demonstration of the three developmental stages of lily (S1, S2, and S3). (B) Extraction and quantification of anthocyanin in lily petals at different stages. (C) Expression trend of *LvbHLLH13*, *LvMYB5*, and related structural genes during lily development. Data are means ( $\pm$ standard deviation) of three biological replicates per construct. Significant variations were determined by the Student's *t*-test (Different letters indicate significant differences ( $p < 0.05$ ) test by least significant difference (LSD), which are calculated by Student's *t*-test ( $p < 0.05$ ). Significance between groups with different letters were all conformed to level).

### 3.2. Functional Analysis of the Transcription Factors *LvMYB5* and *LvbHLLH13*

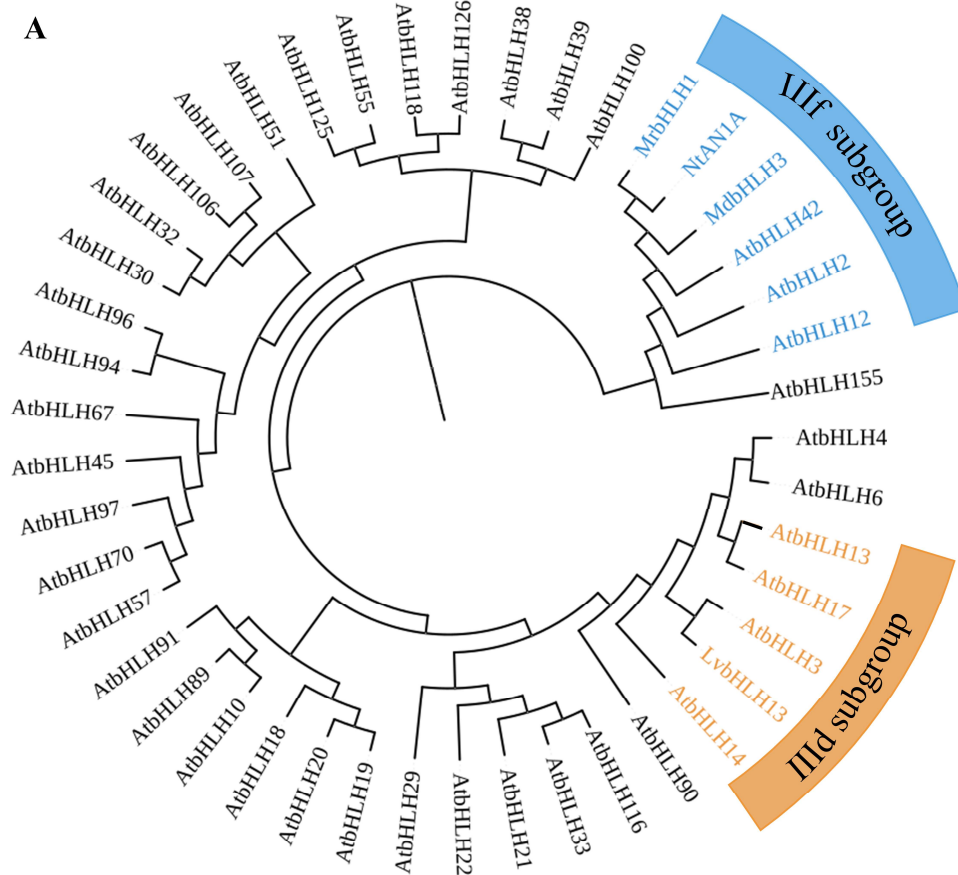
*LvbHLLH13* was cloned to investigate the gene expression dynamics during petal coloring in lily. The cDNA sequence comprises a total length of 1635 base pairs (bp), encompassing the entire open reading frame. Subcellular localization assays demonstrated that the *LvbHLLH13* protein is localized within the nucleus, indicating its role as a nuclear protein (Figure 3).

Figure 3A shows the predicted protein sequences from *LvbHLLH13* and the bHLH gene family in *Arabidopsis thaliana*. The phylogenetic tree demonstrates that *LvbHLLH13* belongs to the *Arabidopsis* bHLH TF IIIId subgroup, which contains four branches of *AtbHLH3*, *AtbHLH13*, *AtbHLH17*, and *AtbHLH14*. In addition, *NtAN1A*, *MrbHLH1*, and *MdbHLH3* were grouped with *AtbHLH42*, *AtbHLH12*, and *AtbHLH2* in the IIIIf subgroup of the *Arabidopsis* bHLH TF family, all having similar functions in activating anthocyanin synthesis [31–33,36,44–49]. Thus, through gene evolutionary analysis, it was preliminary

confirmed that *LvbHLH13* is closely related to other bHLH TFs and plays an important role in the regulation of anthocyanin biosynthesis.



**Figure 2.** Subcellular localization of *LvMYB5*-GFP and *LvbHLH13*-GFP in *N. benthamiana* leaf protoplasts.



**Figure 3.** Cont.

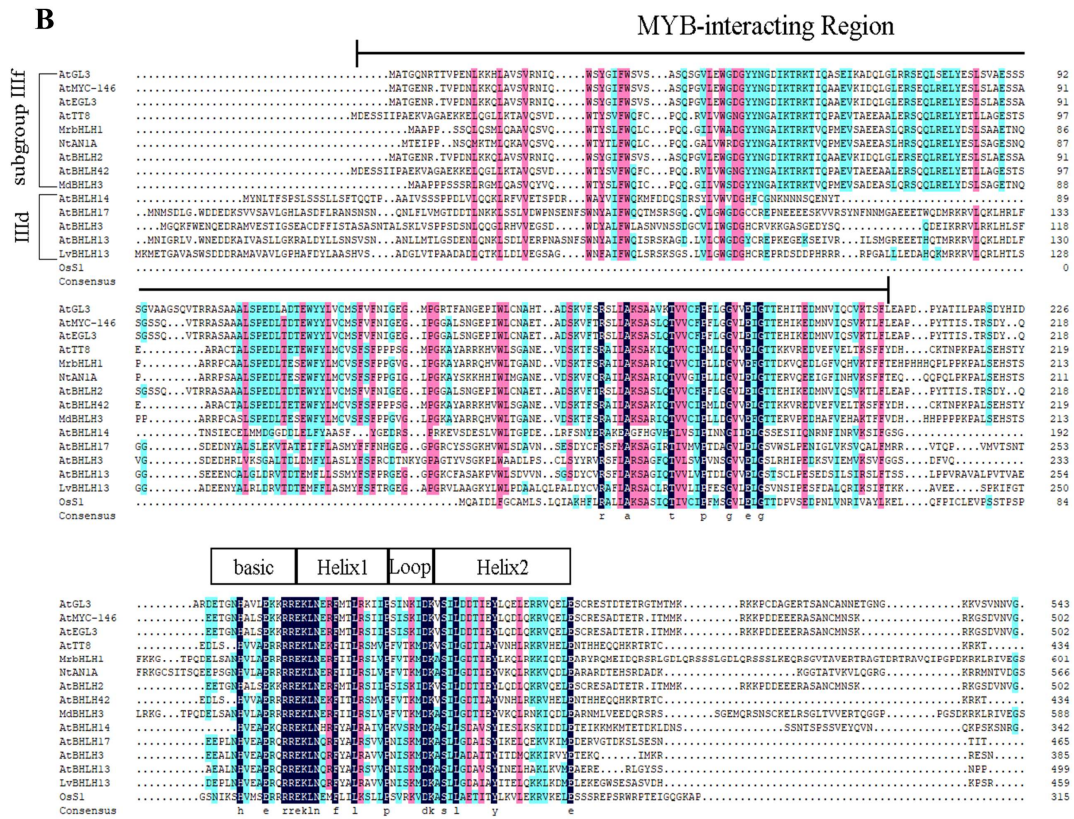


**Figure 3.** Phylogenetic relationships and multi-sequence alignments between *LvbHLLH13* and anthocyanin-related bHLHs in other species. (A) A phylogenetic tree showing the evolutionary relationships between bHLH family proteins from *Arabidopsis*. (B) Multi-sequence alignments of *LvbHLLH13* and the known anthocyanin bHLH regulators in other species. Black lines: MYB interaction; black frame: bHLH domain. Different color stands for ‘sequence homology’ and is an industry standard for sequence matching.

Multiple sequence alignment was performed using the *LvbHLLH13* protein sequence and anthocyanin synthesis-related bHLH TFs from other plants, as shown in Figure 3B. *LvbHLLH13* has similar features to bHLH TFs in many other plants, with all having the common conserved basic-helix1-loop-helix2 domain in common. In addition, IIIc, IIIe, and IIIf subgroups usually have a conserved interaction motif (MIR) that interacts with the MYB protein at the N-terminal region. However, in *LvbHLLH13*, only a few amino acids are conserved. The N-terminal conservatism of the IIIc subgroup is considered an important factor in regulating anthocyanin accumulation. In addition, unlike R proteins, the special function of the III subgroup of the bHLH family is through the regulation of downstream genes. Therefore, the difference in the N-terminal region indicates that *LvbHLLH13* may lack the ability to form the traditional MBW complex and perform the relevant functions [3,4,34].

**3.3. *LvbHLLH13* Gene Silencing Inhibits Anthocyanin Synthesis in Lily Petals**

To elucidate the role of the *LvbHLLH13* gene in anthocyanin production during the development of lily petals, a 273 bp DNA fragment corresponding to the *LvbHLLH13* gene was cloned into the pTRV2 vector for virus-induced gene silencing (VIGS). To avoid the conserved basic-helix1-loop-helix2 domain region of the bHLH gene family, the specific N-terminal region was selected as the cloned fragment (Figure S1). The results of using the recombinant pTRV2 + pTRV1 to infect lily petals are shown in Figure 4. After transfection with the empty TRV vector, the color of lily petals was not significantly affected, but upon transfection with the pTRV2-*LvbHLLH13* vector, bleached color was observed after *LvbHLLH13* silencing. Compared to the region infected with the empty TRV vector, the extracted sample from the region infected with pTRV2-*LvbHLLH13* was visibly lighter in color,



and the anthocyanin content was also significantly reduced (Figure 4B,C). Furthermore, qRT-PCR analysis revealed that the expression levels of *LvbHLH13*, *LvMYB5*, *Lv3GT*, *LvCHS*, *LvDFR*, and *LvF3'H* were downregulated in lily petals infected with the pTRV2-*LvbHLH13* recombinant vector (Figure 4D). The above results indicate that after *LvbHLH13* gene silencing, the expression of related genes was downregulated and anthocyanin accumulation decreased significantly. Hence, it is reasonable to infer that silencing the *LvbHLH13* gene impacts the pigmentation of lily petals by downregulating the expression of genes involved in the anthocyanin biosynthesis pathway.

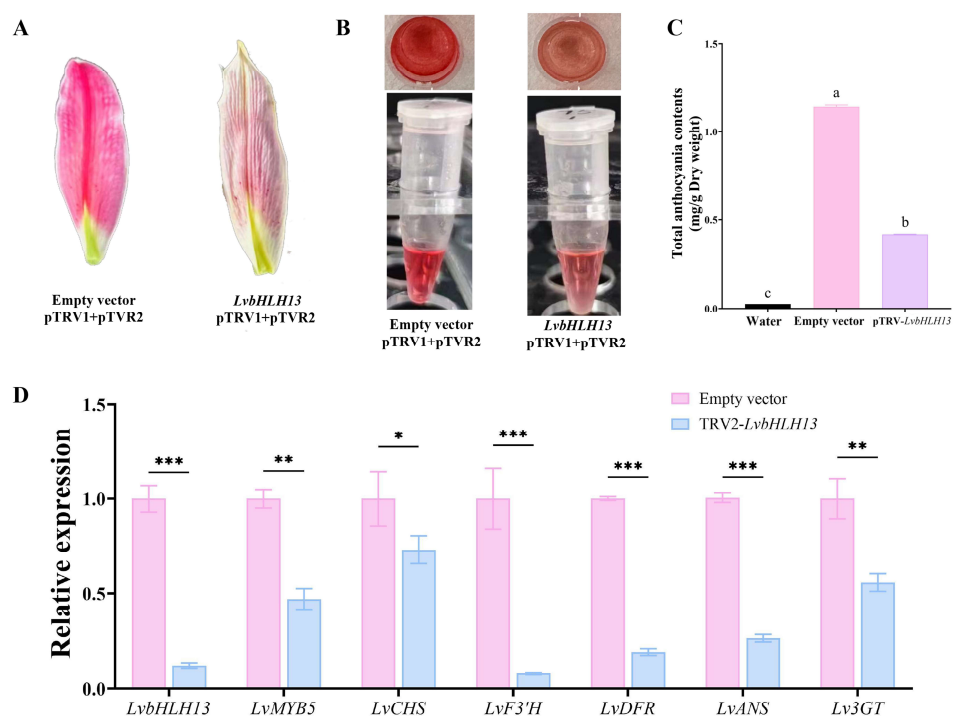


**Figure 4.** Verification of the function of *LvbHLH13* in anthocyanin biosynthesis by virus-induced gene silencing (VIGS). (A,B) Lily petals and their extracted anthocyanins after different treatments. (C) Measurement of total anthocyanin content in lily petals. (D) Expression levels of *LvbHLH13*, *LvMYB5*, and structural genes in lily petals. Data are means ( $\pm$ standard deviation) of three biological replicates per construct. Significant variations were determined by the Student's *t*-test (\*  $p < 0.05$ , \*\*  $p < 0.01$ , \*\*\*  $p < 0.001$ ). Different letters indicate significant differences ( $p < 0.05$ ) test by least significant difference (LSD).

### 3.4. Overexpression of *LvbHLH13* Promotes Anthocyanin Accumulation in Lily Petals

Silencing the *LvbHLH13* gene has already confirmed that it can affect anthocyanin accumulation. To reconfirm this conclusion, transient overexpression was utilized to investigate the underlying mechanisms of *LvbHLH13*. Two groups of *Agrobacterium* suspensions containing empty vectors, 35S::*LvbHLH13*, respectively, were infiltrated into the outer petals of green lily buds that had just begun to pigment, and then darken for one day. After one week, the empty vector group exhibited slight discoloration, indicating that *Agrobacterium* infection had no positive effect on anthocyanin accumulation. However, the petal infiltrated with 35S::*LvbHLH13* had a darker color and higher anthocyanin level than the empty vector control petal (Figure 5A–C).

Using qRT-PCR, we successfully confirmed the gene expression patterns in lily leaves (Figure 5D). Data on anthocyanin synthesis-related structural gene expression revealed that, in contrast to the control group, the transient overexpression of *LvbHLH13* could lead to the upregulation of *LvMYB5*, *LvCHS*, *LvF3'H*, *LvDFR*, *LvANS*, and *Lv3GT* expression. These results further suggest that the overexpression of *LvbHLH13* in lily petals can promote anthocyanin accumulation through *LvMYB5*.

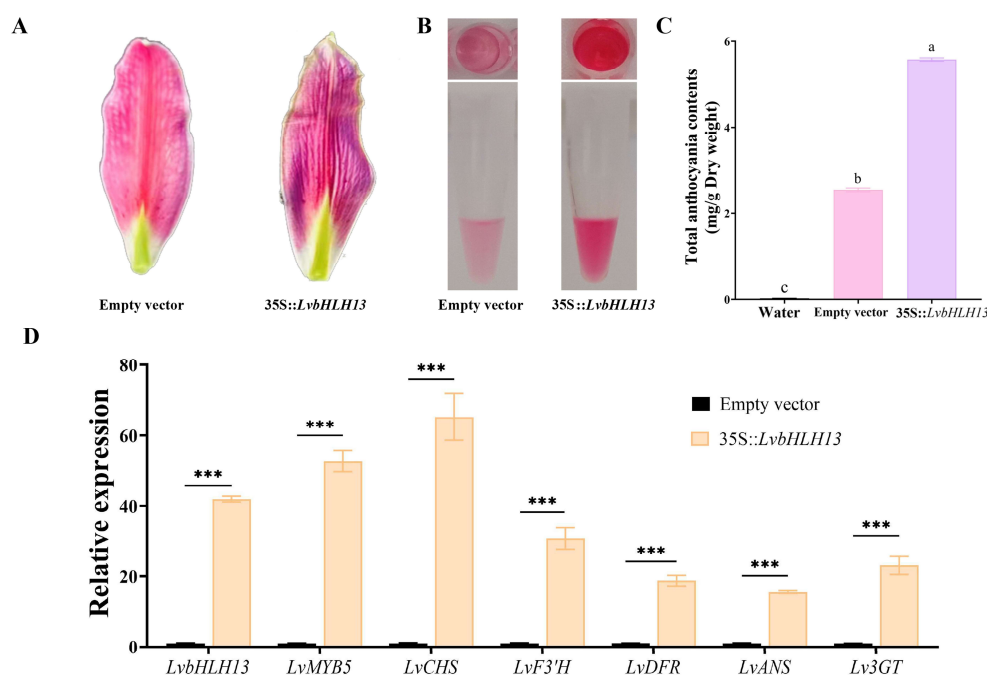


**Figure 5.** The biosynthesis of anthocyanins in *LvbHLH13* overexpression lily. (A) Color change in lily petals of untransformed control and transformation with *LvbHLH13*. (B) Extraction of total anthocyanins in untransformed control and transgenic lily petals. (C) Quantification of total anthocyanin content in lily petals. (D) The expressions of *LvbHLH13*, *LvMYB5*, and related structural genes in the anthocyanin biosynthetic pathway. The vertical bars represent the standard error of triplicate experiments. Data are means ( $\pm$ standard deviation) of three biological replicates per construct. Significant variations were determined by the Student's *t*-test (\*\*\*)  $p < 0.001$ ). Different letters indicate significant differences ( $p < 0.05$ ) test by least significant difference (LSD).

A yeast one-hybrid (Y1H) assay was used to investigate the interaction between *LvbHLH13* and *LvMYB5* in vitro (Figure 6A). The three partial fragments of the MYB promoter, namely, MYBp1 (1–1200 bp), MYBp2 (1–900 bp), and MYBp3 (1–300 bp), were inserted into the *EcoR* I and *Pst* I sites of the pAbAi vector, respectively. None of them displayed autoactivation on an SD/−U/−L medium with 75 ng/mL ABA background lacking uracil and leucine. Then, the bait constructs carrying the pM1/2/4-pabai plasmid vectors were severally co-transformed with pGADT7-*LvbHLH13*, after which normal growth was observed in the yeast cell on the medium (SD/−U/−L with ABA). These results indicate that *LvbHLH13* can physically interact with the sequence of the *LvMYB5* promoter in vitro.

Moreover, EMSA was used to analyze the interaction between the *LvbHLH13* and *LvMYB5* promoter sequences further and identify the binding sites (Figure 6B). The CDS of *LvbHLH13* was cloned into pGEX6P (*LvbHLH13*-GST) and inserted into Rosetta Competent cells (DE3). Three labeled DNA probes (Figure S1) containing the G box in the *LvMYB5* upstream promoter sequence (G1, G2, and G4) were used for detection probes, and unlabeled probes were used as competitors. As shown in Figure 6B, in the presence of both the labeled probe and *LvbHLH13*-GST, the electrophoresis bands shifted, and even when the competitor probe was increased to 100 times, the bias was still produced, indicating the specific binding between *LvbHLH13* and *LvMYB5* promoters.

In order to further investigate whether *LvbHLH13* can affect *LvMYB5* promoter expression in vivo, we developed a dual-luciferase expression vector (Figure 7A). The 2000 bp *LvMYB5* upstream promoter sequence was inserted into the pGreenII-0800-LUC vector to construct the reporter vector *LvMYB5* pro-LUC. The CDS of *LvbHLH13* was cloned into the 35S::GFP vector (*LvbHLH13*-62-SK), using *LvbHLH13*-62-SK and the empty vector (pGreenII-62-SK) as effector carriers. When *LvMYB5* pro-LUC and *LvbHLH13*-62-SK

were co-infiltrated simultaneously, the luciferase activity in *N. benthamiana* leaves was significantly higher than that in leaves co-infiltrated with pGreenII-62-SK and *LvMYB5* pro-LUC alone (as shown in Figure 7B,C). Notably, *LvbHLH13*-62-SK alone did not induce increased activation. These results strongly suggest that *LvbHLH13* interacts with the promoter of *LvMYB5* to synergistically promote the in vivo production of anthocyanins.

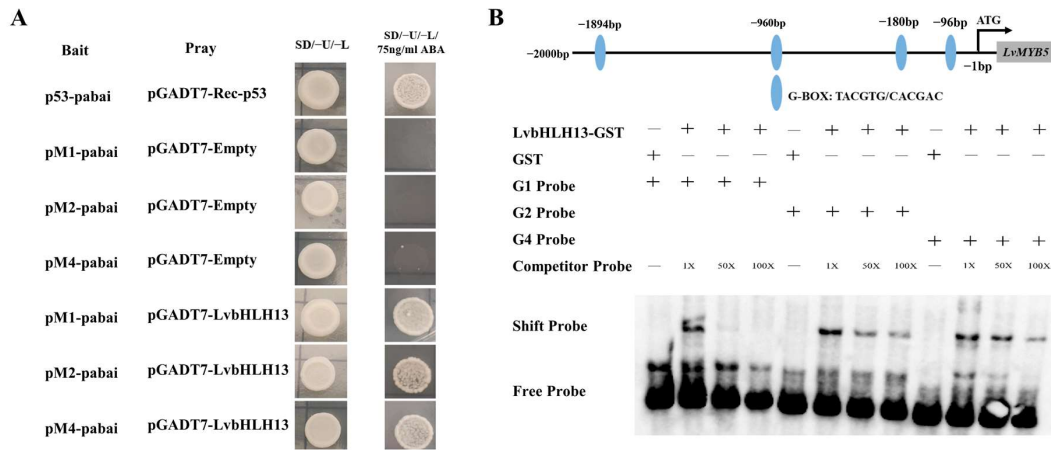


**Figure 6.** Experimental verification of the physical interaction between *LvbHLH13* and *LvMYB5* promoters. **(A)** In vitro interaction of *LvbHLH13* and *LvMYB5* promoter detected in Y1H assays. The yeast strain was co-transformed with the indicated combinations of *LvbHLH13* and *LvMYB5* promoters fused to pGADT7 or pGBKT7. All of the yeast clones were grown on appropriate media to maintain the expression vectors and to test for activation of the reporter gene. The different lengths of the MYB gene are named M1 (1200 bp), M2 (900 bp), and M4 (300 bp). **(B)** Results of the EMSA test on the interaction between *LvbHLH13* and *LvMYB5* sequences. G1, G2, and G4 are the three G-box-labeled DNA probes in the upstream promoter sequence of *LvMYB5*.

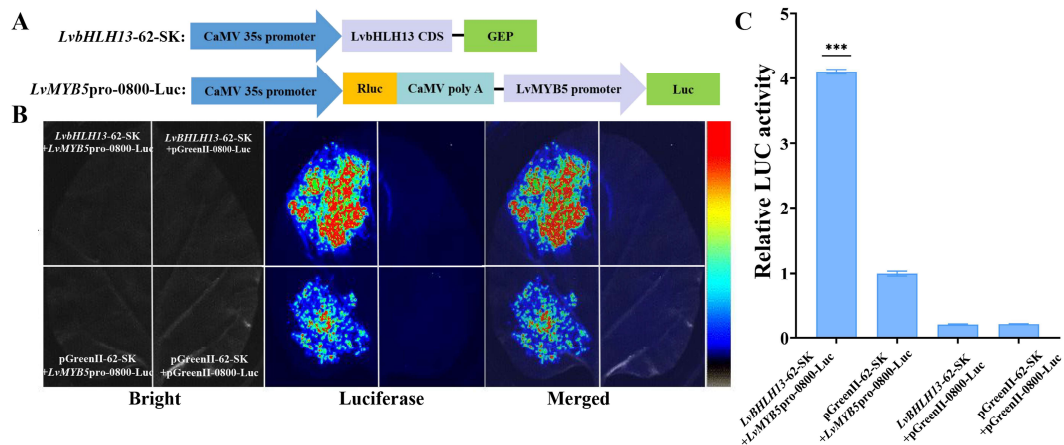


**Figure 7.** In vivo interactions between *LvMYB5* promoter and *LvbHLH13* TFs were verified by using the dual luciferase assay in *N. benthamiana* leaves. **(A)** Schematic diagrams showing the vector constructs. **(B)** Comparison of color changes with different carriers infiltrating under fluorescence. **(C)** Results of luciferase activity detection. Data are means ( $\pm$ standard deviation) of three biological replicates per construct. Significant variations were determined by the Student's *t*-test (\*\* $p < 0.001$ ).

A yeast two-hybrid (Y2H) assay was performed by inserting the CDS of *LvbHLH13* into the *EcoR* I/ *Bam*H I site of pGADT7 and inserting the CDS of *LvMYB5* into the *EcoR* I/ *Pst* I site of pGBKT7 to investigate the interaction between *LvbHLH13* and *LvMYB5*. As shown in Figure S2, normal growth was observed in yeast cells co-transformed with pGBKT7-*LvMYB5* and pGADT7-*LvbHLH13* using SD/-Trp/-Leu media, but their growth was inhibited on SD/-Trp/-Leu/-His/-Ade media. This suggests that *LvbHLH13* is

unable to interact with LvMYB5 to further form the MBW complex, which may be caused by the absence of MIR sequence at the N-terminal region of LvbHLH13.

#### 4. Discussion

Anthocyanins serve as essential contributors to flower growth and development, enhancing their visual allure and nutritional value and providing biological safeguarding. The transcriptional orchestration of structural genes alongside associated transcription factors (TFs) dictates anthocyanin synthesis. Numerous investigations of diverse plant species have underscored the influence of various bHLH TFs in governing anthocyanin or proanthocyanidin production. Noteworthy examples include TT8, GL3, and EGL3 in *Arabidopsis* [32,33]; LcbHLH1 and LcbHLH3 in litchi [50]; and MdbHLH3 and MdbHLH33 in apple [51]. The strawberry R2R3-FaMYB5/FaEGL3/FaLWD1 form a MBW complex, which positively regulates anthocyanin accumulation [25]. *HonAnt2* plays a crucial role in the formation of different qingke barley grain colors [26]. *ThRAX2* may also regulate the transport and activity of the anthocyanidin synthase protein [27]. ICE2 acts antagonistically to control seed dormancy [29]. The burgeoning evidence underscores the pivotal role of bHLH proteins in anthocyanin accumulation. To date, most reported anthocyanin-related bHLHs belong to the IIIf subfamily, with limited studies exploring anthocyanin pathway regulation by other subfamilies, particularly in lilies. In this study, we found that the expression pattern of the bHLH IIIId transcription factor during lily petal coloring correlates with *LvMYB5* expression and anthocyanin accumulation. Despite previous indications of the bHLH IIIId TFs' involvement in various plant development processes and responses to environmental stresses, their specific role in flavonoid biosynthesis in lilies remains underexplored.

In the previous study [37], *LvMYB5*'s ectopic expression was found to enhance pigmentation in lily flowers. *LvMYB5* strongly activated the expression of anthocyanin-related structural genes, leading to increased anthocyanin accumulation. In the present research, we demonstrated that the overexpression of *LvbHLH13* in lily petals regulates pigment accumulation and the expression of the key genes involved in the anthocyanin biosynthesis pathway, including *LvMYB5*, *LvCHS*, *LvF3'H*, *LvDFR*, *LvANS*, and *Lv3GT* (Figures 5 and 6). Conversely, silencing the *LvbHLH13* gene resulted in a significant reduction in the relative anthocyanin content in petals, accompanied by a noticeable discoloration of the infected area. These findings collectively underscore the critical role of *LvbHLH13* in anthocyanin biosynthesis and its specific regulatory relationship with *LvMYB5*.

In our study, the expression of *LvbHLH13* was highest in the S1 period, slightly downregulated in the S2 period, and significantly downregulated in the S3 period. This is consistent with changes in the early anthocyanin biosynthetic gene *LvCHS*, indicating that *LvbHLH13* is mainly expressed during the early stage of anthocyanin accumulation.

*LvbHLH13* has similar features to bHLH TFs in many other plants (Figure 3B). In comparison, IIIId and IIIf subgroups usually have a conserved interaction motif (MIR) that interacts with the MYB protein at the N-terminal region. However, in the IIIId subgroup *LvbHLH13*, a segment of amino acids is mutated (YYNGXIKTRKTXQXXEI-LXRSXQLRELY). The N-terminal conservatism of the IIIId subgroup is considered an important factor in regulating anthocyanin accumulation. Therefore, the difference observed in the N-terminal region indicates that *LvbHLH13* may be different from IIIf subgroups bHLH TFs, which have the ability to form the traditional MBW complex, while performing functions via the regulation of the downstream MYB [3,4,34]. This provides a basis for the study of the bHLH III subgroup in lily.

Lily petals had a bleached color after *LvbHLH13* VIGS silencing. Compared to the region infected with the empty TRV vector, the region infected with pTRV2-*LvbHLH13* was visibly lighter in color, and the anthocyanin content was also significantly reduced (Figure 4B,C). qRT-PCR analysis revealed that the expressions of *LvbHLH13* and related genes were significantly downregulated in lily petals (Figure 4D), and anthocyanin accumulation decreased significantly. Meanwhile, the transient overexpression of *LvbHLH13*

could lead to the upregulated expression of *LvMYB5*, *LvCHS*, *LvF3'H*, *LvDFR*, *LvANS*, and *Lv3GT*. These results further suggest that the overexpression of *LvbHLH13* in lily petals can promote anthocyanin accumulation through *LvMYB5* (Figure 5). These results are consistent with previous studies indicating that the TFs positively regulated anthocyanins in other plants [25,28,37,39,40,50]. This suggests that the bHLH TF family is genetically homogeneous in terms of their functions associated with plant coloration.

*LvbHLH13* is functionally similar to other reported genes in the bHLH TFs family, but its underlying mechanism, as described above, is different from that in most plants. Studies have reported that in the presence of light, *LvCOP1* can facilitate the ubiquitination and degradation of *LvMYB1*, thereby precisely regulating anthocyanin accumulation in lily [40]. We predict that *LvbHLH13* and its upstream *LvCOP1*, may be profoundly linked in regulating anthocyanin.

In summary, the current study reveals a IIIId subfamily bHLH partner of *LvMYB5* that contributes to the regulation of anthocyanin biosynthesis in lily. The expression profile of *LvbHLH13* is different from that of traditional MBW complexes, which interact with the *LvMYB5* promoter to activate its transcription, promoting anthocyanin accumulation. This study reveals a new bHLH candidate and bHLH-MYB partner involved in the anthocyanin regulatory network that need further research. These findings provide valuable insights for breeding lilies with varying anthocyanin contents.

**Supplementary Materials:** The following supporting information can be downloaded at: <https://www.mdpi.com/article/10.3390/horticulturae10090926/s1>, Figure S1: Phylogenetic relationships of the bHLH gene family in lily (*Lilium* 'Viviana'); Figure S2: Experimental verification of the physical interaction between *LvbHLH13* and *LvMYB5* proteins.; Table S1: Primer Sequences.

**Author Contributions:** L.C. developed the research concept and design, which was subsequently implemented by W.A. W.A. conducted the majority of the experiments and assisted with data analysis alongside L.C. D.M. and Z.G., X.L., Q.G. and S.S. also provided valuable input towards generating some of the data. M.Z., with the assistance of Y.S., Y.H. and M.I. and other contributing authors, authored the manuscript. All authors reviewed the manuscript. All authors have read and agreed to the published version of the manuscript.

**Funding:** This research was funded by the China Agriculture Research System (CARS-23) and the Natural Science Foundation of Liaoning Province (2023-BSBA-279) and the National Key R & D Program of China (Grant No. 2019YFD1001002). The APC was funded by the China Agriculture Research System (CARS-23).

**Data Availability Statement:** All relevant data in this study are provided in the article and its Supplementary Figure files, and further inquiries can be directed to the corresponding authors.

**Acknowledgments:** We thank Yule Liu from Tsinghua University and Professor Tao Zhou from T China Agricultural University for providing plasmid *E. coli* and *Agrobacterium*. Thanks to the anonymous reviewers and editors for their quite constructive comments.

**Conflicts of Interest:** The authors declare no competing interests.

## References

- Alappat, B.; Alappat, J. Anthocyanin Pigments: Beyond Aesthetics. *Molecules* **2020**, *25*, 5500. [CrossRef]
- Baudry, A.; Heim, M.A.; Dubreucq, B.; Caboche, M.; Weisshaar, B.; Lepiniec, L. TT2, TT8, and TTG1 synergistically specify the expression of BANYULS and proanthocyanidin biosynthesis in *Arabidopsis thaliana*. *Plant J.* **2004**, *39*, 366–380. [CrossRef] [PubMed]
- Carretero-Paulet, L.; Galstyan, A.; Roig-Villanova, I.; Martínez-García, J.F.; Bilbao-Castro, J.R.; Robertson, D.L. Genome-Wide Classification and Evolutionary Analysis of the bHLH Family of Transcription Factors in *Arabidopsis*, Poplar, Rice, Moss, and Algae. *Plant Physiol.* **2010**, *153*, 1398–1412. [CrossRef] [PubMed]
- Deng, G.-M.; Zhang, S.; Yang, Q.-S.; Gao, H.-J.; Sheng, O.; Bi, F.-C.; Li, C.-Y.; Dong, T.; Yi, G.-J.; He, W.-D.; et al. MaMYB4, an R2R3-MYB Repressor Transcription Factor, Negatively Regulates the Biosynthesis of Anthocyanin in Banana. *Front. Plant Sci.* **2021**, *11*, 600704. [CrossRef] [PubMed]
- Deng, J.; Li, J.; Su, M.; Lin, Z.; Chen, L.; Yang, P. A bHLH gene NnTT8 of *Nelumbo nucifera* regulates anthocyanin biosynthesis. *Plant Physiol. Biochem.* **2021**, *158*, 518–523. [CrossRef]

6. Deng, J.; Wu, D.; Shi, J.; Balfour, K.; Wang, H.; Zhu, G.; Liu, Y.; Wang, J.; Zhu, Z. Multiple MYB Activators and Repressors Collaboratively Regulate the Juvenile Red Fading in Leaves of Sweetpotato. *Front. Plant Sci.* **2020**, *11*, 941. [[CrossRef](#)]
7. Espley, R.V.; Hellens, R.P.; Putterill, J.; Stevenson, D.E.; Kuttuy-Amma, S.; Allan, A.C. Red colouration in apple fruit is due to the activity of the MYB transcription factor, MdMYB10. *Plant J.* **2007**, *49*, 414–427. [[CrossRef](#)]
8. Fernández-Calvo, P.; Chini, A.; Fernández-Barbero, G.; Chico, J.-M.; Gimenez-Ibanez, S.; Geerinck, J.; Eeckhout, D.; Schweizer, F.; Godoy, M.; Franco-Zorrilla, J.M.; et al. The *Arabidopsis* bHLH Transcription Factors MYC3 and MYC4 Are Targets of JAZ Repressors and Act Additively with MYC2 in the Activation of Jasmonate Responses. *Plant Cell* **2011**, *23*, 701–715. [[CrossRef](#)]
9. Hellens, R.P.; Allan, A.C.; Friel, E.N.; Bolitho, K.; Grafton, K.; Templeton, M.D.; Karunairatnam, S.; Gleave, A.P.; Laing, W.A. Transient expression vectors for functional genomics, quantification of promoter activity and RNA silencing in plants. *Plant Methods* **2005**, *1*, 13. [[CrossRef](#)]
10. Hichri, I.; Barrieu, F.; Bogs, J.; Kappel, C.; Delrot, S.; Lauvergeat, V. Recent advances in the transcriptional regulation of the flavonoid biosynthetic pathway. *J. Exp. Bot.* **2011**, *62*, 2465–2483. [[CrossRef](#)]
11. Huang, H.; Gao, H.; Liu, B.; Fan, M.; Wang, J.; Wang, C.; Tian, H.; Wang, L.; Xie, C.; Wu, D.; et al. bHLH13 Regulates Jasmonate-Mediated Defense Responses and Growth. *Evol. Bioinform.* **2018**, *14*, 1176934318790265. [[CrossRef](#)] [[PubMed](#)]
12. Jiang, L.; Yue, M.; Liu, Y.; Zhang, N.; Lin, Y.; Zhang, Y.; Wang, Y.; Li, M.; Luo, Y.; Zhang, Y.; et al. A novel R2R3-MYB transcription factor FaMYB5 positively regulates anthocyanin and proanthocyanidin biosynthesis in cultivated strawberries (*Fragaria × ananassa*). *Plant Biotechnol. J.* **2023**, *21*, 1140–1158. [[CrossRef](#)] [[PubMed](#)]
13. Kim, J.; Kim, D.-H.; Lee, J.-Y.; Lim, S.-H. The R3-Type MYB Transcription Factor BrMYBL2.1 Negatively Regulates Anthocyanin Biosynthesis in Chinese Cabbage (*Brassica rapa* L.) by Repressing MYB–bHLH–WD40 Complex Activity. *Int. J. Mol. Sci.* **2022**, *23*, 3382. [[CrossRef](#)]
14. Lai, B.; Du, L.-N.; Liu, R.; Hu, B.; Su, W.-B.; Qin, Y.-H.; Zhao, J.-T.; Wang, H.-C.; Hu, G.-B. Two LcbHLH Transcription Factors Interacting with LcMYB1 in Regulating Late Structural Genes of Anthocyanin Biosynthesis in *Nicotiana* and *Litchi chinensis* During Anthocyanin Accumulation. *Front. Plant Sci.* **2016**, *7*, 166. [[CrossRef](#)] [[PubMed](#)]
15. Li, H.; Yang, Z.; Zeng, Q.; Wang, S.; Luo, Y.; Huang, Y.; Xin, Y.; He, N. Abnormal expression of bHLH3 disrupts a flavonoid homeostasis network, causing differences in pigment composition among mulberry fruits. *Hortic. Res.* **2020**, *7*, 83. [[CrossRef](#)] [[PubMed](#)]
16. Li, H.; Yao, Y.; An, L.; Li, X.; Cui, Y.; Bai, Y.; Yao, X.; Wu, K. Isolation and expression analysis of the HvnAnt2 gene in qingke barley (*Hordeum vulgare* L. var. *nudum* Hook. f.) varieties with different grain colours. *Czech J. Genet. Plant Breed.* **2024**, *60*, 107–118. [[CrossRef](#)]
17. Liu, X.; Gu, J.; Wang, J.; Lu, Y. Lily breeding by using molecular tools and transformation systems. *Mol. Biol. Rep.* **2014**, *41*, 6899–6908. [[CrossRef](#)]
18. Liu, Y.; Zhang, J.; Yang, X.; Wang, J.; Li, Y.; Zhang, P.; Mao, J.; Huang, Q.; Tang, H. Diversity in flower colorations of *Ranunculus asiaticus* L. revealed by anthocyanin biosynthesis pathway in view of gene composition, gene expression patterns, and color phenotype. *Environ. Sci. Pollut. Res.* **2018**, *26*, 13785–13794. [[CrossRef](#)]
19. Lloyd, A.; Brockman, A.; Aguirre, L.; Campbell, A.; Bean, A.; Cantero, A.; Gonzalez, A. Advances in the MYB–bHLH–WD Repeat (MBW) Pigment Regulatory Model: Addition of a WRKY Factor and Co-option of an Anthocyanin MYB for Betalain Regulation. *Plant Cell Physiol.* **2017**, *58*, 1431–1441. [[CrossRef](#)]
20. Lorenzo, O.; Chico, J.M.; Saénchez-Serrano, J.J.; Solano, R. JASMONATE-INSENSITIVE1 Encodes a MYC Transcription Factor Essential to Discriminate between Different Jasmonate-Regulated Defense Responses in *Arabidopsis*[W]. *Plant Cell* **2004**, *16*, 1938–1950. [[CrossRef](#)]
21. Lotkowska, M.E.; Tohge, T.; Fernie, A.R.; Xue, G.-P.; Balazadeh, S.; Mueller-Roeber, B. The *Arabidopsis* transcription factor MYB112 promotes anthocyanin formation during salinity and under high light stress. *Plant Physiol.* **2015**, *169*, 1862–1880. [[CrossRef](#)]
22. Lu, R.; Li, Y.; Zhang, J.; Wang, Y.; Zhang, J.; Li, Y.; Zheng, Y.; Li, X.-B. The bHLH/HLH transcription factors GhFP2 and GhACE1 antagonistically regulate fiber elongation in cotton. *Plant Physiol.* **2022**, *189*, 628–643. [[CrossRef](#)] [[PubMed](#)]
23. Ma, D.; Constabel, C.P. MYB Repressors as Regulators of Phenylpropanoid Metabolism in Plants. *Trends Plant Sci.* **2019**, *24*, 275–289. [[CrossRef](#)]
24. Marasek-Ciolakowska, A.; Nishikawa, T.; Shea, D.J.; Okazaki, K. Breeding of lilies and tulips—Interspecific hybridization and genetic background. *Breed. Sci.* **2018**, *68*, 35–52. [[CrossRef](#)] [[PubMed](#)]
25. Mekapogu, M.; Vasamsetti, B.M.K.; Kwon, O.-K.; Ahn, M.-S.; Lim, S.-H.; Jung, J.-A. Anthocyanins in Floral Colors: Biosynthesis and Regulation in Chrysanthemum Flowers. *Int. J. Mol. Sci.* **2020**, *21*, 6537. [[CrossRef](#)]
26. Mrkvicová, E.; Pavlata, L.; Karásek, F.; Štátník, O.; Doležalová, E.; Trojan, V.; Kizek, R.; Holeksová, V.; Mareš, J.; Brabec, T.; et al. The influence of feeding purple wheat with higher content of anthocyanins on antioxidant status and selected enzyme activity of animals. *Acta Vet. Brno* **2017**, *85*, 371–376. [[CrossRef](#)]
27. Muhammad, N.; Uddin, N.; Khan, M.K.U.; Ali, N.; Ali, K.; Jones, D.A. Diverse role of basic Helix-Loop-Helix (bHLH) transcription factor superfamily genes in the fleshy fruit-bearing plant species. *Czech J. Genet. Plant Breed* **2023**, *59*, 1–13. [[CrossRef](#)]
28. Nakata, M.; Ohme-Takagi, M. Two bHLH-type transcription factors, JA-ASSOCIATED MYC2-LIKE2 and JAM3, are transcriptional repressors and affect male fertility. *Plant Signal. Behav.* **2014**, *8*, e26473. [[CrossRef](#)]
29. Nesi, N.; Debeaujon, I.; Jond, C.; Pelletier, G.; Caboche, M.; Lepiniec, L. The TT8 Gene Encodes a Basic Helix-Loop-Helix Domain Protein Required for Expression of DFR and BAN Genes in *Arabidopsis Siliques*. *Plant Cell* **2000**, *12*, 1863–1878. [[CrossRef](#)]

30. Nguyen, C.T.; Tran, G.B.; Nguyen, N.H. The MYB–bHLH–WDR interferers (MBWi) epigenetically suppress the MBW’s targets. *Biol. Cell* **2019**, *111*, 284–291. [[CrossRef](#)]
31. Qi, T.; Song, S.; Ren, Q.; Wu, D.; Huang, H.; Chen, Y.; Fan, M.; Peng, W.; Ren, C.; Xie, D. The Jasmonate-ZIM-Domain Proteins Interact with the WD-Repeat/bHLH/MYB Complexes to Regulate Jasmonate-Mediated Anthocyanin Accumulation and Trichome Initiation in *Arabidopsis thaliana*. *Plant Cell* **2011**, *23*, 1795–1814. [[CrossRef](#)] [[PubMed](#)]
32. Fonseca, S.; Fernández-Calvo, P.; Fernández, G.M.; Díez-Díaz, M.; Gimenez-Ibanez, S.; López-Vidriero, I.; Godoy, M.; Fernández-Barbero, G.; Van Leene, J.; De Jaeger, G.; et al. bHLH003, bHLH013 and bHLH017 Are New Targets of JAZ Repressors Negatively Regulating JA Responses. *PLoS ONE* **2014**, *9*, e86182. [[CrossRef](#)] [[PubMed](#)]
33. Shin, J.; Park, E.; Choi, G. PIF3 regulates anthocyanin biosynthesis in an HY5-dependent manner with both factors directly binding anthocyanin biosynthetic gene promoters in *Arabidopsis*. *Plant J.* **2007**, *49*, 981–994. [[CrossRef](#)]
34. Silva, S.; Costa, E.M.; Calhau, C.; Morais, R.M.; Pintado, M.E. Anthocyanin extraction from plant tissues: A review. *Crit. Rev. Food Sci. Nutr.* **2015**, *57*, 3072–3083. [[CrossRef](#)]
35. Sun, Y.; Zhang, Y.; Ni, N.; Wang, B.; Chen, J.; Sun, S.; Han, W.; Zhang, X.; Muhammad, I.; Chen, L.; et al. Interplay between LvCOP1 and LvMYB1 governs light-induced anthocyanin biosynthesis in lily (*Lilium ‘Viviana’*). *Sci. Hortic.* **2024**, *332*, 113197. [[CrossRef](#)]
36. Tao, R.; Yu, W.; Gao, Y.; Ni, J.; Yin, L.; Zhang, X.; Li, H.; Wang, D.; Bai, S.; Teng, Y. Light-Induced Basic/Helix-Loop-Helix64 Enhances Anthocyanin Biosynthesis and Undergoes CONSTITUTIVELY PHOTOMORPHOGENIC1-Mediated Degradation in Pear. *Plant Physiol.* **2020**, *184*, 1684–1701. [[CrossRef](#)]
37. Tominaga-Wada, R.; Iwata, M.; Nukumizu, Y.; Wada, T. Analysis of IIIId, IIIe and IVa group basic-helix-loop-helix proteins expressed in *Arabidopsis* root epidermis. *Plant Sci.* **2011**, *181*, 471–478. [[CrossRef](#)]
38. Wang, J.; Cao, K.; Wang, L.; Dong, W.; Zhang, X.; Liu, W. Two MYB and Three bHLH Family Genes Participate in Anthocyanin Accumulation in the Flesh of Peach Fruit Treated with Glucose, Sucrose, Sorbitol, and Fructose In Vitro. *Plants* **2022**, *11*, 507. [[CrossRef](#)] [[PubMed](#)]
39. Wang, L.; Tang, W.; Hu, Y.; Zhang, Y.; Sun, J.; Guo, X.; Lu, H.; Yang, Y.; Fang, C.; Niu, X.; et al. A MYB/bHLH complex regulates tissue-specific anthocyanin biosynthesis in the inner pericarp of red-centered kiwifruit *Actinidia chinensis* cv. Hongyang. *Plant J.* **2019**, *99*, 359–378. [[CrossRef](#)]
40. Wang, Y.; Wu, J.; Li, J.; Liu, B.; Wang, D.; Gao, C. The R2R3-MYB transcription factor ThRAX2 recognized a new element MYB-T (CTTCCA) to enhance cadmium tolerance in *Tamarix hispida*. *Plant Sci.* **2023**, *329*, 111574. [[CrossRef](#)]
41. Xu, F.; Tang, J.; Wang, S.; Cheng, X.; Wang, H.; Ou, S.; Gao, S.; Li, B.; Qian, Y.; Gao, C.; et al. Antagonistic control of seed dormancy in rice by two bHLH transcription factors. *Nat. Genet.* **2022**, *54*, 1972–1982. [[CrossRef](#)] [[PubMed](#)]
42. Yamagishi, M. How genes paint Lily flowers: Regulation of colouration and pigmentation patterning. *Sci. Hortic.* **2013**, *163*, 27–36. [[CrossRef](#)]
43. Yamagishi, M.; Shimoyamada, Y.; Nakatsuka, T.; Masuda, K. Two R2R3-MYB Genes, Homologs of Petunia AN2, Regulate Anthocyanin Biosyntheses in Flower Tepals, Tepal Spots and Leaves of Asiatic Hybrid Lily. *Plant Cell Physiol.* **2010**, *51*, 463–474. [[CrossRef](#)]
44. Yan, H.-X.; Fu, D.-Q.; Zhu, B.-Z.; Liu, H.-P.; Shen, X.-Y.; Luo, Y.-B. Sprout vacuum-infiltration: A simple and efficient agroinoculation method for virus-induced gene silencing in diverse solanaceous species. *Plant Cell Rep.* **2012**, *31*, 1713–1722. [[CrossRef](#)] [[PubMed](#)]
45. Yin, X.; Lin, X.; Liu, Y.; Irfan, M.; Chen, L.; Zhang, L. Integrated metabolic profiling and transcriptome analysis of pigment accumulation in diverse petal tissues in the Lily cultivar ‘Vivian’. *BMC Plant Biol.* **2020**, *20*, 446. [[CrossRef](#)] [[PubMed](#)]
46. Yin, X.; Zhang, Y.; Zhang, L.; Wang, B.; Zhao, Y.; Irfan, M.; Chen, L.; Feng, Y. Regulation of MYB Transcription Factors of Anthocyanin Synthesis in Lily Flowers. *Front. Plant Sci.* **2021**, *12*, 761668. [[CrossRef](#)]
47. Yu, C.; Huang, J.; Wu, Q.; Zhang, C.; Li, X.-L.; Xu, X.; Feng, S.; Zhan, X.; Chen, Z.; Wang, H.; et al. Role of female-predominant MYB39-bHLH13 complex in sexually dimorphic accumulation of taxol in *Taxus media*. *Hortic. Res.* **2022**, *9*, uhac062. [[CrossRef](#)]
48. Yu, H.; Song, S.; Qi, T.; Fan, M.; Zhang, X.; Gao, H.; Huang, H.; Wu, D.; Guo, H.; Xie, D. The bHLH Subgroup IIIId Factors Negatively Regulate Jasmonate-Mediated Plant Defense and Development. *PLoS Genet.* **2013**, *9*, e1003653.
49. Yu, J.Q.; Gu, K.D.; Sun, C.H.; Zhang, Q.Y.; Wang, J.H.; Ma, F.F.; You, C.X.; Hu, D.G.; Hao, Y.J. The apple bHLH transcription factor MdbHLH3 functions in determining the fruit carbohydrates and malate. *Plant Biotechnol. J.* **2020**, *19*, 285–299. [[CrossRef](#)]
50. Zhang, F.; Gonzalez, A.; Zhao, M.; Payne, C.T.; Lloyd, A. A network of redundant bHLH proteins functions in all TTG1-dependent pathways of *Arabidopsis*. *Development* **2003**, *130*, 4859–4869. [[CrossRef](#)]
51. Zhang, L.; Duan, Z.; Ma, S.; Sun, S.; Sun, M.; Xiao, Y.; Ni, N.; Muhammad, I.; Chen, L.; Sun, Y. SIMYB7, an AtMYB4-Like R2R3-MYB Transcription Factor, Inhibits Anthocyanin Accumulation in *Solanum lycopersicum* Fruits. *J. Agric. Food Chem.* **2023**, *71*, 18758–18768. [[CrossRef](#)] [[PubMed](#)]

**Disclaimer/Publisher’s Note:** The statements, opinions and data contained in all publications are solely those of the individual author(s) and contributor(s) and not of MDPI and/or the editor(s). MDPI and/or the editor(s) disclaim responsibility for any injury to people or property resulting from any ideas, methods, instructions or products referred to in the content.